Article

JOURNAL OF COMPOSITE MATERIALS

Journal of Composite Materials
45(23) 2465–2473

DOI: 10.1177/0021998311401105
jcm.sagepub.com

SAGE

Effective thermal conductivity of silicone/phosphor composites

Qin Zhang[1,2], Zhihua Pi[2,3], Mingxiang Chen[1,2], Xiaobing Luo[2,4], Ling Xu[5] and Sheng Liu[1,2]

Abstract

The effective thermal conductivity of silicone/phosphor composites is studied experimentally and numerically. Thermal conductivity measurements are conducted from 30°C to 150°C for the composites with phosphor volume fraction up to 40%. In the numerical study, a finite element model with empirical particle size distribution and random particle position is constructed using a probability density function and the Monte Carlo method, and the interfacial thermal resistance layer between phases also introduced in the model. The results indicate that when phosphor concentration is below 25 vol.%, the conductivity of the composite increases slightly with either phosphor volume fraction or temperature, and the Kapitza radius of the composite is 0.8 μm. When phosphor concentration is above 25 vol.%, the increase of conductivity correlates positively with phosphor volume fraction significantly but negatively with the temperature, and the Kapitza radius is 0.032 μm.

Keywords

silicone/phosphor composites, thermal conductivity, particle size distribution, interface thermal resistance

Introduction

Composites of silicone matrix filled with the phosphors, as a light converting layer, have unique applications in high-power light-emitting diodes (HP-LED), which are projected to comprise a 100 billion USD lighting market within 10 years to come. Selection or development of silicone/phosphor composite for HP-LED is subject to several criteria. Besides the criterion of achieving appropriate optical properties for the phosphor layer, some thermal properties have to be satisfied because of the concern of the coefficient of thermal expansion mismatch and to avoid excessive temperature buildup. Bonding of phosphor particles and the silicone and the interface of the composites to the chip surface and the silicone is also a big concern. One key thermal property is thermal conductivity. To the best of the authors' knowledge, the thermal conductivity of silicone/phosphor composite in solid-state lighting (SSL) has not been well analyzed in the literature, in part due to the ignorance of academic community with regard to this highly proprietary nature of this industry. But with the drive for more green energy and lighting, SSL becomes more and more important. With the current performance of white light converted by the yellow phosphors on blue chips exceeding more than 100 Lm/W, there is no question that SSL will eventually replace conventional lighting. Therefore, a more fundamental understanding of thermal properties is essential.

Many previous studies focused on the theoretical analysis of thermal conductivity of structural

[1]Institute of Microsystems, School of Mechanical Science and Engineering, Huazhong University of Science & Technology, Wuhan 430074, China.
[2]Division of MOEMS, Wuhan National Lab for Optoelectronics, Wuhan 430074, China.
[3]School of Optoelectronics Science and Engineering, Huazhong University of Science & Technology, Wuhan 430074, China.
[4]School of Energy and Power Engineering, Huazhong University of Science & Technology, Wuhan 430074, China.
[5]School of Material Science and Engineering, Huazhong University of Science & Technology, Wuhan 430074, China.

Corresponding author:
Sheng Liu, Institute of Microsystems, School of Mechanical Science and Engineering, Huazhong University of Science & Technology, Wuhan 430074, China
Email: victor_liu63@126.com

composites and developed a number of theoretical models. For examples, the Maxwell[1] and Bruggeman[2] equations represented how the thermal conductivity of a composite depends, at low and high filler concentrations, respectively, on the thermal conductivity and the volume fraction of each component of the composite. Based on the equations above, Hasselman and Johnson,[3] Benveniste,[4] and A.G. Every et al.[5] established the expressions which consider the effect of filler size and interface thermal resistance. Taking account of both the effect of interface thermal resistance and the radii of filler along every axis, Nan et al.[6] developed a more general effective medium approach formulations which can be applied to arbitrary particulate composites.

Apart from theoretical models mentioned above, numerical simulation methods such as finite element method have proven to be powerful tools to investigate the thermal conductivity of composites. To simulate the heat conduction across the composites, many computational models have been established. These models have the sphere,[7] ellipsoid,[8] plate,[9] rod,[10] or polyhedron[8] fillers distributed in a cubic unit cell. In general, the fillers are distributed in the unit cell randomly[11,12] or inside a cubic crystal structure like atoms.[7] As far as these computational models are concerned, it is important to determine the particle size distribution which has a significant impact on the effective thermal conductivity of a composite. In the early literature, the fillers in a unit cell are of the same size. However, in general, the size of fillers is not fixed but distributed in some range, which is due to manufacturing process capability limits. In fact, to improve the maximum packing fraction in the composite, it is necessary to use particles with a large distribution size that extends over several orders of magnitude.[13] Hence some computational models with fillers of different size emerged in recent years. Although these models are superior to the ones with fixed size of fillers, they are still not good enough in the sense that the filler size distributions in these models are assumed to obey some specific probability density function (PDF) such as logarithmic normal distribution,[14] which do not correspond with empirical size distribution.

Based on the existing theory and numerical simulation method, this article investigates how the effective thermal conductivity of silicone/phosphor composite relates to the temperature and the phosphor concentration by both experiment, and finite element modeling which overcomes the shortcomings of the existing ones. The numerical results are compared with theoretical models and experimental results. The temperature jumps across the phosphor–silicone interface are also presented and analyzed.

Experimental procedures

Materials

High optical transparency silicone is used as matrix, and Ce^{3+} doped YAG ($Y_3Al_5O_{12}$) powder as filled phosphor particles. The densities of the phosphor and silicone are 4.8 g/cm^3 and 1.1 g/cm^3, respectively. The thermal conductivity of the phosphor is 13W/m K. Figure 1 shows the typical scanning electron microscope (SEM) image of the phosphor particles. The phosphor particles are different in size and therefore it is necessary to determine the size distribution. The empirical distribution of the phosphor size provided by the manufacturer is shown in Figure 2. The mean size of phosphor particles is 13.0 ± 2.0 μm in diameter.

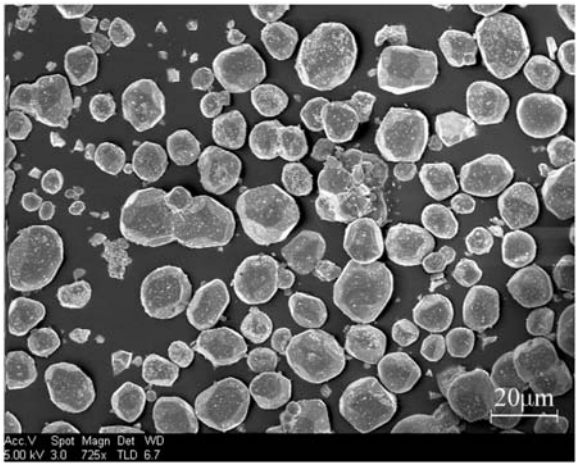

Figure 1. A typical SEM image of the phosphor particles.

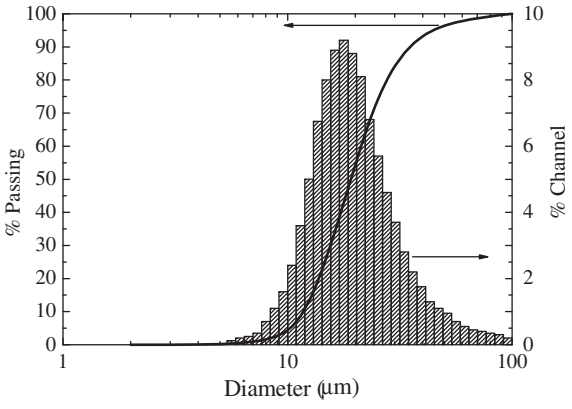

Figure 2. Empirical particle size distribution: the percentage of particles in individual size intervals (filled bars) and the cumulative distribution curve (continuous line).

Processing of composites

The silicone/phosphor composites are prepared by mixing uncured silicone with phosphor powders at various volumetric concentrations. The filler volume fraction V_f is defined as follows:[11]

$$V_f = \frac{V_{phosphor}}{V_{phosphor} + V_{silicone}} \quad (1)$$

where $V_{phosphor}$ is the volume of phosphor fillers and $V_{silicone}$ that of the silicone matrix. To remove air bubbles, the mixture is placed in a vacuum pressure chamber until no bubbles emerge. Then, composite samples (with diameter 17.5 mm and thickness 2 mm) are cured at 150°C for 1 h.

Measurement

Laser flash method is used to measure the thermal conductivity of the composites. The 'static' thermal diffusivity, α_s, is measured by LFA 447 NanoFlash. A schematic diagram of the test method is shown in Figure 3. The lower surface of the specimen is heated by flash laser source, and the transient temperature on the upper surface is monitored with an infrared detector. The 'static' thermal diffusivity in the temperature range from 30°C to 150°C is measured in air. The effective thermal conductivity K^* and the 'static' thermal diffusivity are related by the following equation:[15]

$$K^* = \alpha_s(\rho c)_e \quad (2)$$

where $(\rho c)_e$ is the effective volumetric specific heat of composites.

Numerical simulation

Geometry modeling

The fillers are treated as spherical particles of different diameters. A Monte Carlo code is developed to generate the diameters according to the empirical particle size distribution. First, the probability distribution is determined by calculating the derivative of empirical cumulative distribution data. By fitting for the probability distribution curve with segmented function, the PDF of particle size is obtained as follows:

$$f(x) = \begin{cases} \frac{100}{15.5\sqrt{\pi/2}} \exp\left(-2\left(\frac{x-16}{8.5}\right)^2\right) & x \le 9.6 \\ 6 - 6/\left(1 + \exp\left(\frac{x-10.8}{1.2}\right)\right) & 9.6 < x \le 9.8 \\ 0.3 + 5.5\exp\left(-\exp\left(\frac{x-15.6}{6.3}\right) - \frac{x-15.6}{6.3} + 1\right) & 9.8 < x \le 20.6 \\ 0.08 + \frac{6.1}{1+(x/24.5)^{5.8}} & x > 20.6 \end{cases} \quad (3)$$

where x is the diameter of particles as random variable and $f(x)$ the PDF of x. Figure 4 displays the empirical probability distribution and the fitted curves. Then, using the developed Monte Carlo code, random numbers based on Equation (3) are generated until the needed volume fraction is met. A typical retrieved particle size distribution compared with the curve of PDF is also shown in Figure 4.

The Monte Carlo method is also applied to generate the coordinate of the center of the randomly distributed fillers on condition that the unit cell has close-packed structure and the fillers have hard cores, which means they cannot overlap or contact each other. According to the literature,[10] the insufficient filler numbers in the unit cell can greatly reduce the precision of the numerical results, especially at low filler concentrations. Therefore, for all the computational models, more than 100 particles are generated and dispersed in the unit cell so that the sample variance of thermal conductivity is about $1.25 \times 10^{-5} W^2/m^2 \cdot K^2$ (sample size $n = 60$). A cubic cell model with random position of fillers and empirical distribution of filler size is shown in Figure 5.

Boundary conditions

It is well known that, due to the imperfect contact, there exists interfacial thermal resistance between the phases of a composite. Compared with the other dimensions, the interface layer between the phases is very thin, so that heat cannot flow directly through the layer, which results in a temperature jump across the interface.

To take the interfacial thermal resistance mentioned above into account in our calculations, the boundary condition of the thin thermal resistive layer is applied to the interior boundaries between the particles and matrix for the computational cell model. The interfacial thermal property is characterized by Kapitza radius, a_k, which is defined as:[6]

$$a_k = K_m \cdot \lim_{\substack{\delta \to 0 \\ K_s \to 0}} (\delta / K_s) \quad (4)$$

where K_m is the thermal conductivity of the matrix, and, δ and K_s the thickness and conductivity of the

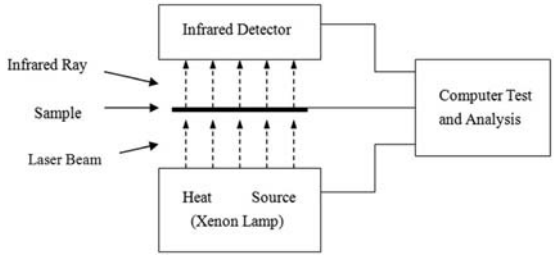

Figure 3. Schematic of laser flash method to measure thermal diffusivity.

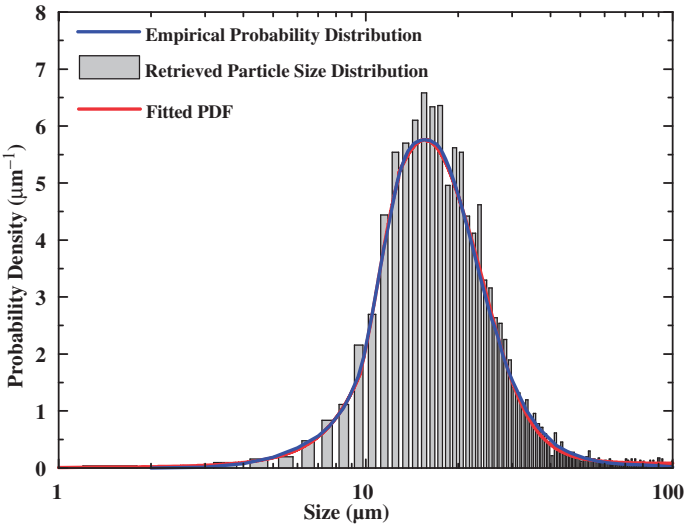

Figure 4. A typical Monte Carlo method retrieved particle size distribution (filled bars) and the analytical PDF of particle size (continuous line).

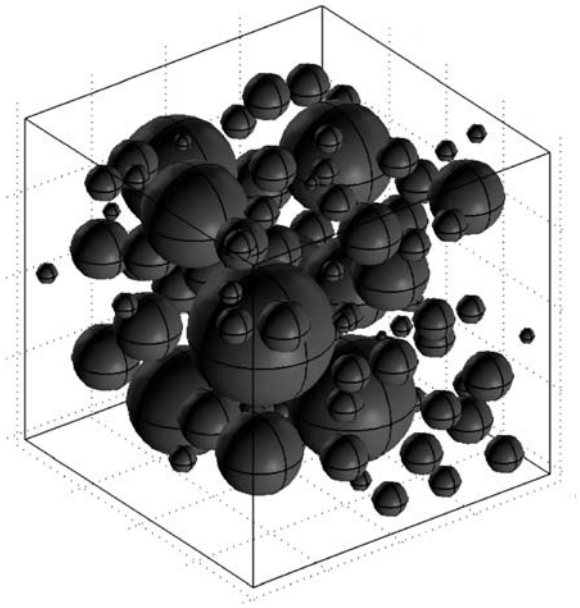

Figure 5. A typical unit cell model.

interface layer surrounding the filler, respectively. Generally, $0 \leq a_k \leq \infty$, with $a_k = 0$ corresponding to the perfect interface. For $a_k > 0$, temperature jumps across the interface.[6] In addition, the Kapitza radius is in principle the critical particle size. If the filler particle radius a is smaller than the Kapitza radius, the thermal conductivity of composites will be lower than that of the matrix, and it will decrease as the filler fraction increases.[16]

Assuming that the layer is a thin film with a constant thickness and that tangential heat flux in the layer is negligible, the temperature jump across the boundary becomes proportional to the normal heat flux. Hence, two separate but symmetric heat flux boundary conditions for thermal resistive layer can be expressed as:[17]

$$\begin{aligned} -n_{\text{down}} \cdot (-K_{\text{down}} \nabla T_{\text{down}}) &= \frac{K_s}{\delta}\left(T_{\text{up}} - T_{\text{down}}\right) \text{ on } \partial\Omega_{\text{down}} \\ -n_{\text{up}} \cdot \left(-K_{\text{up}} \nabla T_{\text{up}}\right) &= \frac{K_{\text{s}}}{\delta}\left(T_{\text{down}} - T_{\text{up}}\right) \text{ on } \partial\Omega_{\text{up}} \end{aligned} \tag{5}$$

where n_{up} and n_{down} are, respectively, the normal vector of up and down sides of the boundary, and, δ and K_s the thickness and conductivity of the interface layer surrounding the filler, respectively. From Equation (5), we know that only the factor K_s/δ is needed. This factor can be derived by Equation (4). The correct interfacial thermal conductivity can be specified by considering the thickness of the interface as a very small constant and thus

$$K_s = K_m \delta / a_k \tag{6}$$

The boundary conditions on the external boundaries of the cubic cell model are shown in Figure 6. Heat flux boundary conditions are applied to a pair of parallel surfaces of the cubic cell. A certain heat flux flows into one surface, and in order that heat dissipation takes place, high convection heat transfer coefficient is applied to the other surface. The other four surfaces

are considered as adiabatic to obtain the directional thermal conductivity.

Thermal conductivity calculation

Based on Fourier's law for steady-state heat conduction, the effective thermal conductivity K^* of the composites can be expressed by:

$$K^* = q\frac{\Delta z}{T_1 - T_2} \tag{7}$$

where q is the heat flux through the model, Δz the distance the heat flow through, and T_1 and T_2 the average temperatures of the surfaces which heat flows into and out of, respectively.

Results and discussions

Experimental results

Figure 7 shows the microstructures of fracture surfaces of composites which are observed by scanning electron microscopy. It can be found in the SEM images that the particles are well uniformly embedded in the matrix at 15.8 vol.%. At 25 vol.%, the particles are close to each other and form clusters, as observed in Figure 7(b), which indicates that conductive chains in the composite form.

The thermal conductivity values from 30°C to 150°C of composites for different phosphor volume fractions are shown in Figure 8. Noted that 0% volume fraction represents pure silicone. The figure clearly shows that at constant temperature, higher the volume fraction, higher the thermal conductivity. Until 15.8 vol.%, the increase of conductivity is slight, but above 25 vol.%, the conductivity increases by a fairly big margin with increasing volume fraction. This phenomenon can be explained by percolation theory. In the case of low filler content, the particles are well dispersed and isolated with each other in the matrix, as shown in Figure 7(a). When the filler content increases to 25 vol.%, some particles are interconnected and form conductive chains, as shown in Figure 7(b). These networks increase the conductivity rapidly.

Figure 8 also indicates that at there is a pronounced dependence of the thermal conductivity on the temperature at high filler content. The thermal conductivity of composite decreases with increasing temperature at high concentrations above 25 vol.%. The generally negative temperature dependence was also found by Hasselman and Donaldson[18] and Mu et al.[19] for silicone/ZnO composites. This may be due to the fact that thermal expansion of the silicone matrix widens the distance between fillers and then cuts or shortens some conductive chains, resulting in a decrease in the thermal conductivity of composite. Thermal conductivity increases slightly with increasing temperature at low concentrations from 0 to 15.8 vol.%.

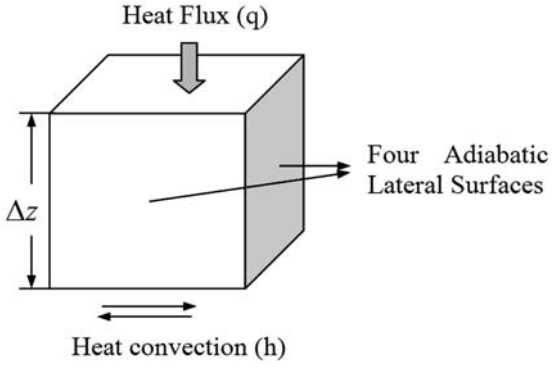

Figure 6. Heat conduction boundary conditions for the cubic cell model.

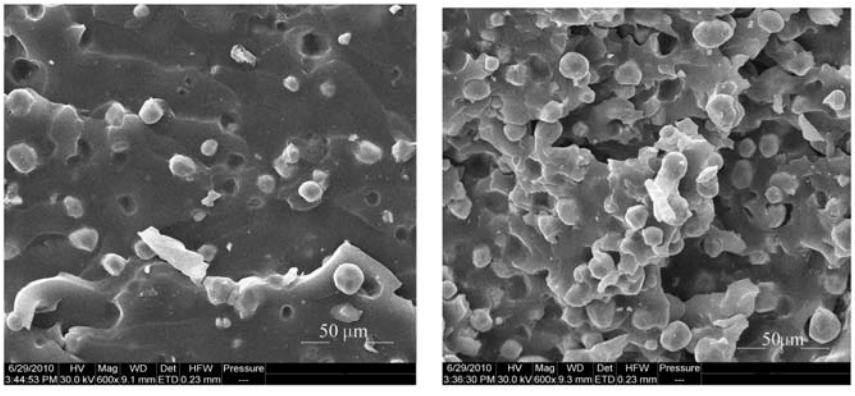

Figure 7. SEM images of phosphor particles embedded in a silicone matrix: (a) 15.8 vol.% and (b) 25 vol.% phosphor containing.

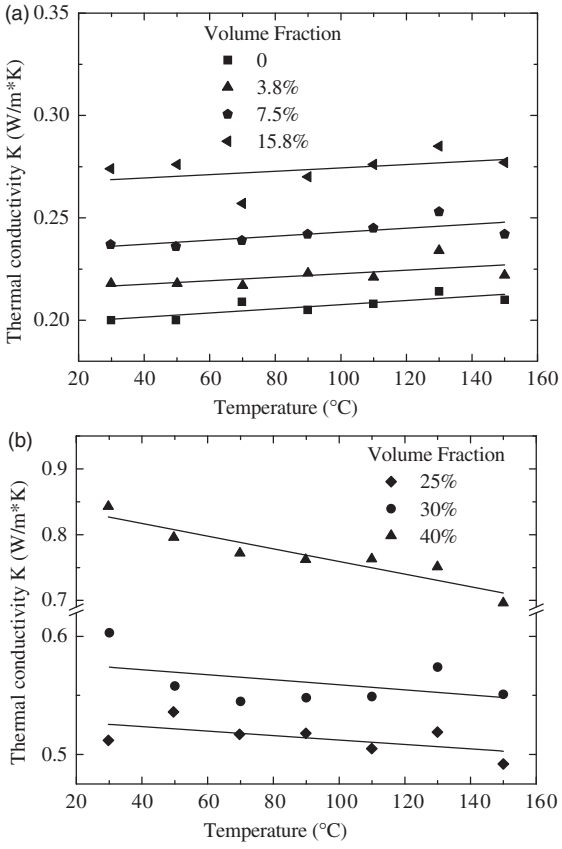

Figure 8. Thermal conductivity from 30°C to 150°C of silicone/phosphor composites for different phosphor volume fractions V_f: (a) low concentrations from 0 to 15.8 vol.%; (b) high concentrations from 25 to 40 vol.%. The solid line shows the linear fit of the data.

Kapitza radius

The Kapitza radius of the composite is derived from comparing the value of effective thermal conductivity predicted by theory with the measured ones. Many models[3–6] have been proposed to predict the effective thermal conductivity K^* of a composite, which take the interfacial thermal resistance and particle size effect into consideration. In view of the fact that each of these models cannot be used for composites with an arbitrary volume fraction but rather for ones with a volume fraction in a certain range, this study adopts two models dealing with the case of low volume fraction and of high volume fraction. The two models are as follows:

Hasselman and Johnson model[3,4] for low volume fraction

$$K^* = K_m \frac{K_f(1+2\alpha) + 2K_m + 2V_f[K_f(1-\alpha) - K_m]}{K_f(1+2\alpha) + 2K_m - V_f[K_f(1-\alpha) - K_m]} \quad (8)$$

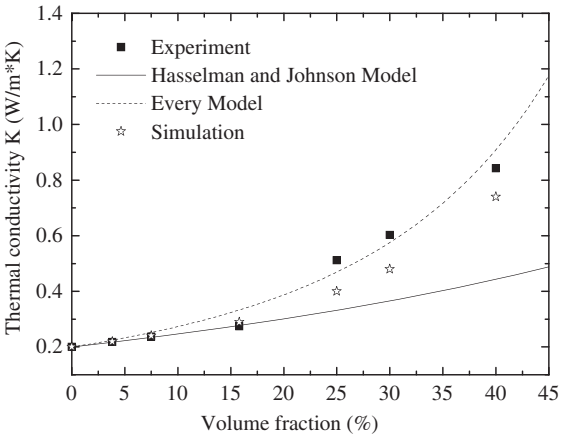

Figure 9. Thermal conductivity of phosphor/silicone composites as a function of volume fraction of phosphor at 30°C.

The model by Every[5] for high volume fraction

$$\frac{K^*}{K_m} = \frac{1}{(1-V_f)^{3(1-\alpha)/(1+2\alpha)}} \quad (9)$$

where K_f is the thermal conductivity of the fillers, and α represents the particle size and interface effect, a non-dimensional parameter, which defined as the following formula:[5,6]

$$\alpha = a_k / r \quad (10)$$

where r is the mean value of radius for the fillers.

By means of minimizing the deviations between the measured values and the ones predicted by the model, nonlinear curve fitting is applied to determine the value of parameter α. By least-square algorithm, it is found that the value of α is about 0.1 for low concentrations and 0.004 for high concentrations. At lower concentrations, the value of α is lower than the one at higher concentrations, which may be a result of direct contact between particles that will shorten the acoustic mismatch resistance and would account for the interfacial thermal resistance decreasing at higher concentrations.[20] As seen from Figure 9, with $\alpha = 0.1$, Equation (8) predicts well for low concentrations from zero to 15.8 vol.%, and with $\alpha = 0.004$, Equation (9) shows good agreement with experimental results for high concentrations from 25 to 40 vol.%. By Equation (10), the value of Kapitza radius a_k is obtained, which is equal to 0.8 μm for low and 0.032 μm for high concentrations.

Numerical simulation results

Assuming that the thickness of the interface layer is 0.01 μm, the interfacial thermal conductivity

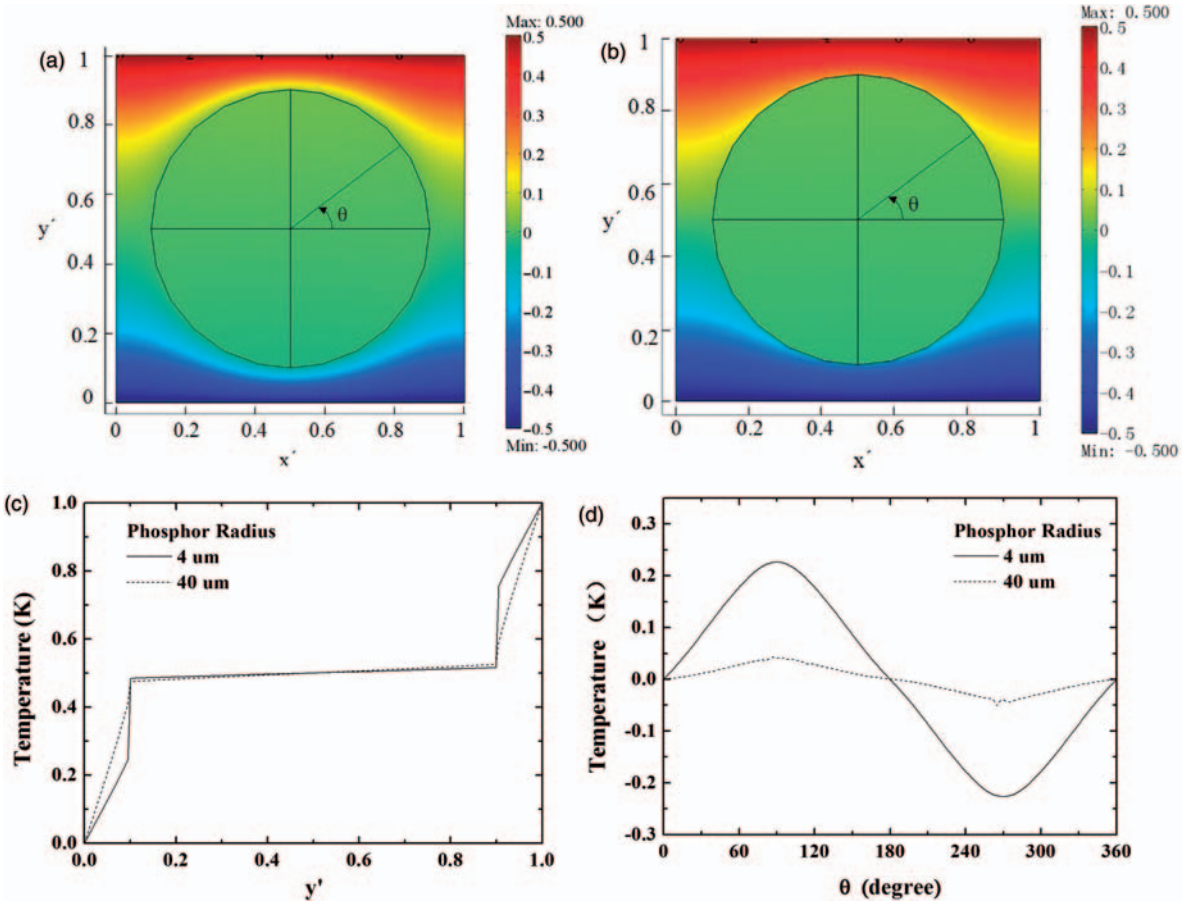

Figure 10. Effective temperature distribution of silicone/phosphor composites with Kapitza radius $a_k = 0.8\,\mu m$: (a) temperature contour for phosphor radius is 40 μm, (b) temperature contour for phosphor radius is 4 μm, (c) temperature distribution along y' axis at $x' = 0.5$, and (d) the temperature jump across silicone/phosphor interface, as a function of the position on the interface. The black circle represents the boundary of phosphor particle.

$K_s = 2.5 \times 10^{-3}$W/m·K for low volume fraction and 6.25×10^{-2}W/m·K for high volume fraction are obtained using the value of Kapitza radii and Equation (6). Adding the interfacial thermal resistance to the interfaces between phosphor particles and silicone matrix permits calculation of the effective conductivity of composites, K^*, which takes into account the interface effect. For one model, K^* is the average of data in three axes.

The K^* obtained by simulation is also shown in Figure 9. At low concentrations up to 15.8 vol.%, the simulated values agree well with the experimental results. At higher concentrations, the numerical values are lower than the experimental ones, perhaps because the hard core algorithm does not allow the direct contacts between particles, which will result in no conductive chains forming in a unit cell. Therefore, silicone matrix plays a major role in the heat transfer process. The silicone matrix is a relatively poor thermal conductor, which leads to lower conductivity of the composite and would account for the discrepancy of experimental and numerical results.

Temperature distribution at the interfaces

To better understand the effect of interfacial thermal resistance, the temperature distributions of silicone/phosphor composites for a particle radius are 4 μm and 40 μm, respectively, are calculated, with the Kapitza radius a_k being 0.8 μm. Figure 10(a) and 10(b) show the temperature contour in the slice along the heat flux flow direction and through the center of the particle. The temperature drop across the thickness of the composites is assumed to be 1 K. The effective temperature distributions are made dimensionless using normalization method. Axial temperature distribution along y' direction at certain fixed x' positions is shown in Figure 10(c). Included in the plot (Figure 10(d)) are the temperature jumps T_{jump} across the interface along the boundary of phosphor particle. Here, T_{jump} is

calculated by subtracting the temperature of silicone at the interface from that of phosphor.

Comparision of Figure 10(a) with 10(c) shows that a large temperature gradient occurs only in the matrix zones located near the top and bottom surfaces of phosphor particle, and that the temperature gradient becomes larger with particle size becoming smaller. The axial temperature plots of the two structures (Figure 10(c)) illustrate that there exists a significant temperature jump across the interfaces between phosphor and silicone. Apparent temperature jumps at the whole interface are clearly shown in Figure 10(d). Although particles have the same Kapitza radius, the larger the particle size, the lower the temperature jump relative to the total temperature difference across the model. In this case, the interfacial thermal resistance will retard less heat transfer of composites, thus increasing the thermal conductivity. Figure 10(d) also indicates that the temperature jumps across the interface layer are not constant because the temperature jump depends on temperature and heat flux, as reported by Struchtrup and Weiss.[21]

Conclusion

The effective thermal conductivity of silicone/phosphor composites is studied experimentally and numerically. Using a laser flash technique, the conductivity with phosphor volume fraction up to 40% and temperature from 30°C to 150°C are obtained. An accurate model is constructed by using the Monte Carlo method. The model development makes it possible to consider the effect of empirical particle size distribution and interfacial thermal resistance. Based on the experimental and numerical analysis, the following conclusions can be drawn as follows:

1. With increasing phosphor concentration, the effective thermal conductivity of silicone/phosphor composites increases. The Hasselman and Johnson model agrees fairly well with the thermal conductivity data at low concentration, and the Every model at high concentration.
2. Above 25 vol.% phosphor, with increasing volume fraction, there is a fairly large increase in conductivity. A phosphor concentration above 25 vol.% should be used in HP-LEDs to increase power dissipation.
3. Below 15.8 vol.% phosphor, the thermal conductivities increase slightly with temperature. Above 25 vol.% phosphor, there is a pronounced negative dependence of thermal conductivities and temperature.
4. A composite with a low phosphor concentration has higher interfacial thermal resistance than a composite with a high phosphor concentration. The Kapitza radii are 0.8 μm for low concentrations and 0.032 μm for high concentrations.
5. There are apparent temperature jumps at the interface. The larger the particle size, the lower the temperature jump relative to the total temperature difference and thus the higher the conductivity of the composites.

Acknowledgments

This study is supported by Nature Science Foundation of China (NSFC) Key Project under grant no. 50835005, National High Technology Research Plan of China (863 Project) under grant no. 2009AA03A1A3. The authors also thank Xiao Jia, Ju Liu, Zhicheng Lv, and Zhangming Mao for stimulating discussions.

References

1. Maxwell JC. *Treatise on electricity and magnetism*. Oxford: Clarendon Press, 1873.
2. Bruggeman DAG. Berechnung verschiedener physikalischer konstanten von heterogenen substanzen. *Ann Phys* 1935; 416(7): 636–664.
3. Hasselman DPH and Johnson LF. Effective thermal conductivity of composites with interfacial thermal barrier resistance. *J Compos Mater* 1986; 21(6): 508–515.
4. Benveniste Y. Effective thermal conductivity of composites with a thermal contact resistance between the constituents: nonduute case. *J Appl Phys* 1987; 61(8): 2840–2843.
5. Every AG, Tzou Y, Hasselman DPH and Raj R. The effect of particle size on the thermal conductivity of ZnS/diamond composites. *Acta Metall Mater* 1992; 40(1): 123–129.
6. Nan CW, Birringer R, Clarke David R and Gleiter H. Effective thermal conductivity of particulate composites with interfacial thermal resistance. *J Appl Phys* 1997; 81(10): 6692–6699.
7. Yue C, Zhang Y, Hu Z, Liu J and Cheng Z. Modeling of the effective thermal conductivity of composite materials with FEM based on resistor networks approach. *Microsyst Technol* 2010; 16(4): 633–639.
8. Zeng J and Fu R. Numerical simulation of thermal conductivity of particle filled epoxy composites. *J Electron Packag* 2009; 131(4): 041006-1–041006-7.
9. Hill RF and Strader JL. Rudimentary finite element thermal modeling of platelet-filled polymer-ceramic composites. *IEEE Trans Compon Packag Technol* 2007; 30(2): 235–241.
10. Foygel M, Morris RD, Anez D, French S and Sobolev VL. Theoretical and computational studies of carbon nanotube composites and suspensions: electrical and thermal conductivity. *Phys Rev B: Condens Matter* 2005; 71(10): 104201-1–104201-8.
11. Sanada K, Tada Y and Shindo Y. Thermal conductivity of polymer composites with close-packed structure of

nano and micro fillers. *Compos Part A* 2009; 40(6–7): 724–730.
12. Smith PA and Torquato S. Computer simulation results for bounds on the effective conductivity of composites media. *J Appl Phys* 1989; 65(3): 893–900.
13. Boudenne A, Ibos L, Fois M, Majesté JC and Géhin E. Electrical and thermal behavior of polypropylene filled with copper particles. *Compos Part A* 2005; 36(11): 1545–1554.
14. Cai WZ, Tu ST and Tao GL. Thermal conductivity of PTFE composites with three-dimensional randomly distributed fillers. *J Thermoplast Compos Mater* 2005; 18(3): 241–253.
15. Pitchumani R and Yao SC. Evaluation of transverse thermal diffusivity of unidirectional fiber-reinforced composites. *Int J Heat Mass Transfer* 1991; 35(9): 2185–2194.
16. Wang J and Yi XS. Effects of interfacial thermal barrier resistance and particle shape and size on the thermal conductivity of AlN/PI composites. *Compos Sci Technol* 2004; 64(10–11): 1623–1628.
17. COMSOL Multiphysics 3.5. COMSOL Multiphysics help document.
18. Hasselman DPH, Donaldson KY and Geiger AL. Effect of reinforcement particle size on the thermal conductivity of a particulate-silicon carbide-reinforced aluminium matrix composite. *J Am Ceram Soc* 1992; 75(11): 3137–3140.
19. Mu Q, Feng S and Diao G. Thermal conductivity of silicone rubber filled with ZnO. *Polym Compos* 2007; 28(2): 125–130.
20. Garrett KW and Rosenberg HM. The thermal conductivity of epoxy-resin/powder composite materials. *J Phys D: Appl Phys* 1974; 7(9): 1247–1258.
21. Struchtrup H and Weiss W. Temperature jump and velocity slip in the moment method. *Continuum Mech Thermodyn* 2000; 12(1): 1–18.